P.Srinivas*

J. Electrical Systems 11-1 (2015): 76-88

Regular paper

Design and FE Analysis of BLDC Motor for Electro-Mechanical Actuator

JES
Journal of Electrical Systems

This paper presents the design of Surface Mounted BLDC Motor for Electro-mechanical actuator. The Electro-mechanical actuators are extensively used in aerospace and defence industry. The preferred motor for such applications is BLDC motor as it is compact in size, offers high speed operation and has high torque to inertia ratio, high efficiency etc. Motor is designed analytically to meet the given specifications of the actuator. The designed motor is verified by conducting Finite Element Analysis (FEA) on the dimensions obtained through analytical calculations. The FEA is conducted on no load and on loaded condition of the motor. The armature reaction effects mainly demagnetizing and cross magnetizing effects on the permanent magnet are analyzed. Finally non-linear FEA concludes that flux, flux density and magnetizing force etc. in various parts of the motor are in the specified limits and motor meets the desired specifications.

Keywords: BLDC Motor; Electromechanical Actuator; Finite Element Analysis

Article history: Received 24 September 2014, Received in revised form 2 December 2014, Accepted 27 December 2014

1. Introduction

Actuators are the integral part of any automated operation of the systems. Many types of actuators like Hydraulic, Pneumatic and Electro-mechanical actuators are used in defence and aerospace industry. Electromechanical (EM) actuators are extensively use in various applications. They are used both in ground as well as airborne systems. The linear EM actuators are used for erection and levelling systems in ground equipment and for aerodynamic /thrust vector control in missile systems [1-3]

BLDC motors are preferred motors for these actuators because of advantages such as high power density, compactness, high torque to inertia ratio, high speed operation etc [1,2]. These motors are fed from the on board/ground DC supply and are controlled based on the torque demand and feedbacks generated in the given application. Design of BLDC motor for rotary Electro-mechanical actuator is designed in [3]. The design is based on high magnetic and electrical loading to get peak torque[4].

Electro-mechanical(EM) actuators call for special design of the motor. This project deals with Electromagnetic design of the motor through analytical approach. As per the requirment of the actuator stack length of 110 mm and stator diameter of 110 mm is selected. Hence, a design is to be developed according to the given specifications. To validate the design of the motor, FE analysis is conducted on no load and on loaded motor. FE analysis is performed by ANSYS software. The effect of armature reaction on the permanent magnet is analysed.

2. Analytical Design and Analysis

The design of Permanent Magnet Brushless DC motor (PM-BLDC motor) for an Electro-mechanical actuator includes selection of initial configuration of the motor, Sizing of motor, magnetic design, electrical design and Non linear magnetic analysis for

*Corresponding author: P.Srinivas, Department of Electrical Engineering, University College of Engineering, Osmania University, Hyderabad-500007, India,, E-mail: srinivasp.eedou@gmail.com

optimization of design. Baseline specifications for the design are derived from the servo system specifications, actuator specifications and mechanical design. Also complete servo system is to be housed in a block within the space provided and weight specified. The base line input parameters taken are from the system specifications and the mechanical design are summerised as follows in the Table 1.

Table 1. Design inputs

Sno	Parameter	Specification
1	Nominal voltage	85 Volts
2	Paek torque	25 N-m
3	Rated torque	18 N-m
4	Max RPM	4000 rpm
5	Motor Stack Length	110 mm
6	Stator Outer Diameter	110 mm
7	Time of operation	5 min(300 sec)

3. Selection of Initial configuration

Among the available Axialflux and Radial flux rotor topologies, the Radial flux topology is selected as the length of the motor here is not so resticted. In view of the advantages of higher flux density and ease of manufacturing, Surface mount PM arrangement is chosen for the current design among the available configurations of the placement of magnets on rotor.

The speed of the motor in this application is expected to be very high. If less number of poles are selected the back iron increaseas. Hence, 8 poles are seleced for the current design in view of the high speed and low volume requirements of the motor**.** In order to reduce cogging torque 3 slots per pole are chosen which will result in 24 stator slots for placing the stator three phase winding. The selection of permanent magnet is based on Max Energy product and operating temparature. Samarium cobalt (Sm2Co17) grade 26 is selected for this application.The slection of soft magnetic material for the core and back iron is based on the permeability, saturation flux density and resistivity. Cobalt-iron alloy is selected for this application.

3.1 Sizing of the motor

Now the overall dimensions of the motor are derived from the required torque the motor is expected to produce. The first step of this process is to arrive at the main dimensions of the motor. These dimensions are constrained by the application in which the actuator is used.To meet the required torque demanded by the motor, the two important parameters which play vital role are electrical loading and magnetic loading. These two are assumed and are justified in the process of magnetic and electrical design of the motor[4-6].

The active motor length can be increased to improve the force generated. However, doing so will increase the mass and volume of the motor. A further consequence is that the resistive loss also increases, since longer slots need longer wire. Therefore, increasing the motor active length does not improve power density or efficiency. As a result, motor length is often choosen as the minimum value required to meet a force specification.In this case the Stack length of the motor 'Li' = 110 mm isconsidered.

As a first step in sizing the motor magnetic loading or Air gap flux density (Bg) and electrical loading (A) will be assumed. Since Smarium Cobalt magnets are selected and surface mounting is assumed for the rotor, the Air gap flux density ie, magnetic loading Bg

can be taken as 0.75 to 0.95 times Br. Hence, magnetic loading is taken as Bg = 0.8 T(Taking $Bg = 0.75\ Br$)

For contunuos rating Brushed DC machines of 5 kW allowed electrical loading is 20000 AT/m. In this case the motor is without brushes and also short time rated hence the value is assumed as 90000 AT/m. Air gap length of 0.5 mm is assumed to meet the manufacturing tolerances. The other dimensions like stator back iron width, stator teeth width and slot area will be calculated after solving the magnetic circuit for airgap flux.

4. Development of Magnetic design

Magnetic equivalent circuit was solved to arrive at parameters like air gap flux density, magnet operating point. During sizing of motor magnetic loading (air gap flux density) was assumed as 0.8T. Because the flux density profile in the air gap will not be trapizoidal but will be distorted due to slot openings. Hence, the air gap flux density cannot be same as calculated from the analytical method but will be less[4,5]. Finite Element Analysis (FEA) will help in assessing the realistic value and helps in validating the design. Some of the parameters calculated are shown below. The parameters of magnetic circuit design are shown in Table 2.

4.1 Area of the Airgap (Ag)

Area of the Airgap is given by

$$Ag = r' \times \theta \times \pi/180 \times Li \tag{1}$$

where ‘r’ is the rotor radius and ‘θ’ is the pole arc

4.2 Airgap permeance

Air gap reluctance is given by

$$R_g = g^{'} \div \mu_0 \times Ag \tag{2}$$

where $g^{'}$ is the modified airgap length

4.3 Internal leakage permeance

Area of the magnet is given by

$$A_m = r \times \theta_m \times \frac{\pi}{180} \times L_i \tag{3}$$

Internal leakage Permeance is

$$P_{mo} = \mu_0 \mu_R L_i \, \theta_p \left(\frac{1}{2} + \frac{r_i}{l_m}\right) \tag{4}$$

$l_m = Lenght\ of\ the\ Magnet$

It is generally considered that $l_m \geq 5 - 6\ g$ (5)

4.4 Tooth thickness (w_{tb})

If there are ‘ N_{tm}' teeth per pole, the airgap flux from each magnet travels through N_{tm} teeth. Therefore each tooth carries $1/N_{tm}$ of air gap flux. If the flux density allowed in the teeth is also B_{max}, then the required tooth width is

$$W_{tb} = \frac{\emptyset_g}{N_{tm} B_{max} K_{st} L_i} \tag{6}$$

Table 2 Magnetic design

S no	Parameter	Value
1	Air gap length (g)	0.5 mm
2	Magnet radial thickness (l_m)	3 mm
3	Air gap flux ($\emptyset_g$)	1.7 mWb
4	Air ap flux density (B_g)	0.8564 T
5	Magnet flux density (B_m)	0.8754 T
6	Magnet MMF (H_m)	140.8 KA/m
7	Magnet Permeance coefficent (PC)	4.95
8	Rotor outer radius	23 mm
9	Stator and rotor back iron (W_{bi})	4.5 mm
10	Tooth thickness (W_{tb})	3 mm

5. Electrical parameters.

The electrical parameters of the BLDC motor include resistance, inductance, back emf, and current. Based on these copper and iron losses which contribute to temparature rise in the motor are found. With this the class of insulation and operating temparature range of magnets is verified. Procedure for calculation of some of the parameters is shown below. All the parameters calculated are shown in Table 3.

5.1 Self Inductance

The inductance of the phase winding is related to the energy stored in the magnetic field generated solely by current flowing in the winding. Since rotor magnets generate flux independent of the winding current, they do not contribute to the self inductance.
The total self inductance of the winding per phase is found by adding airgap self, stack leakage inductance and end turn leakage inductance these components.

$$L_{ph} = No\ of\ slots/ph(L_g + L_s + L_{es}) \tag{7}$$

Where *Lg, Ls and Les* is the airgap self inductance slot leakage inductance and end turn leakage inductance respectively.

Table 3 Electrical parameters

S.no	Parameter	Value
1	Motor Torque constant (K_t)	0.2N-m/Amp
2	Motor Back emf constant (K_b)	0.2 V/rad/sec
3	Armature resistance per phase (R_{ph})	0.011 ohms
4	Inductance per phase (L_{ph})	0.197 mH

6. Finite Element Analysis (FEA) at No load

Finite Element Analysis is used to analyse magnetic circuits arrived by analytical approach in order to get more exact solutions. Using FEA models flux densities and torques can be calculated. Results can be output in various forms including plots of vector magnetic potentials, flux density maps and flux paths [6]. The analysis is performed at no-load to examine the demagnetising effects of airgap and stator slots on the magnet.

The air gap flux density is the parameter which defines the speed and torque capability of the machine. The airgap flux density should be a trapezoidal waveform but due to the slot openings dips will be there in the waveform as shown in Fig. 1. The average flux density from the graph will be below 0.792 T. The two dips in the profile are due to the increased reluctance of two slots openings facing the magnet.

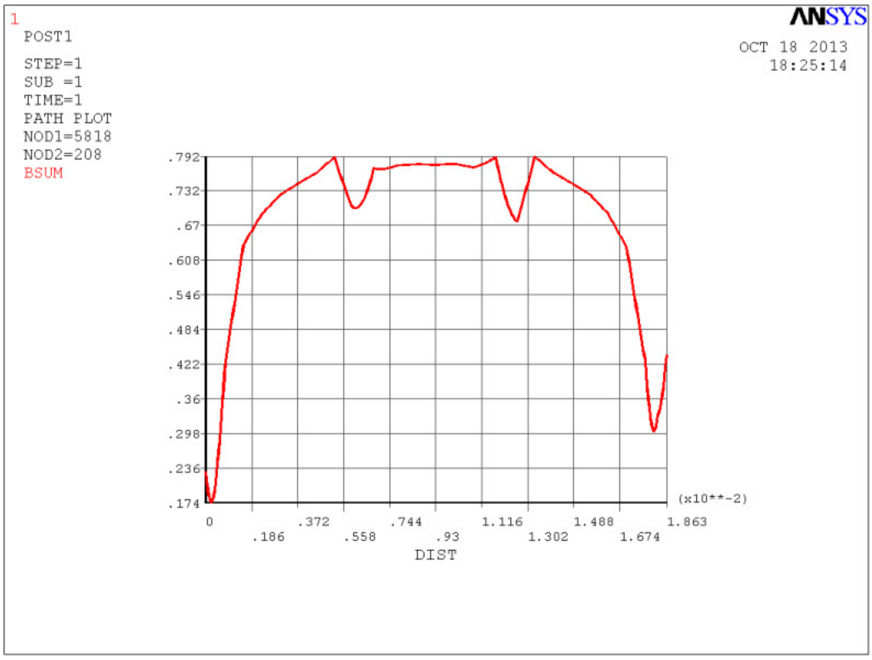

Fig. 1 Airgap flux density at no load

The core flux density in the stator and rotor determines utilisation of core material and hysterisis loss. The flux density in the core is kept below 1.9T to avoid saturation during load conditions. The flux and flux density profiles of the core are shown in Fig. 2 and Fig. 3 respectively.

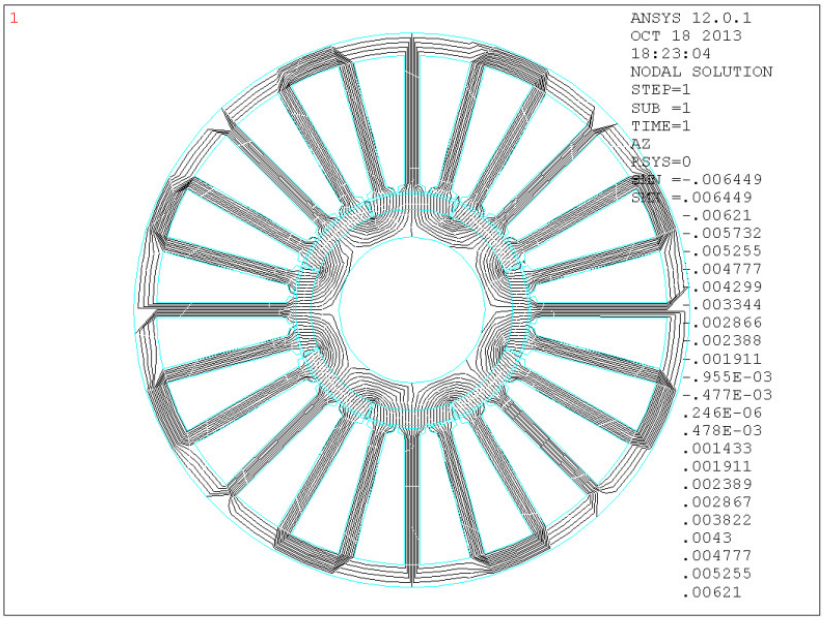

Fig. 2 No load flux in stator core

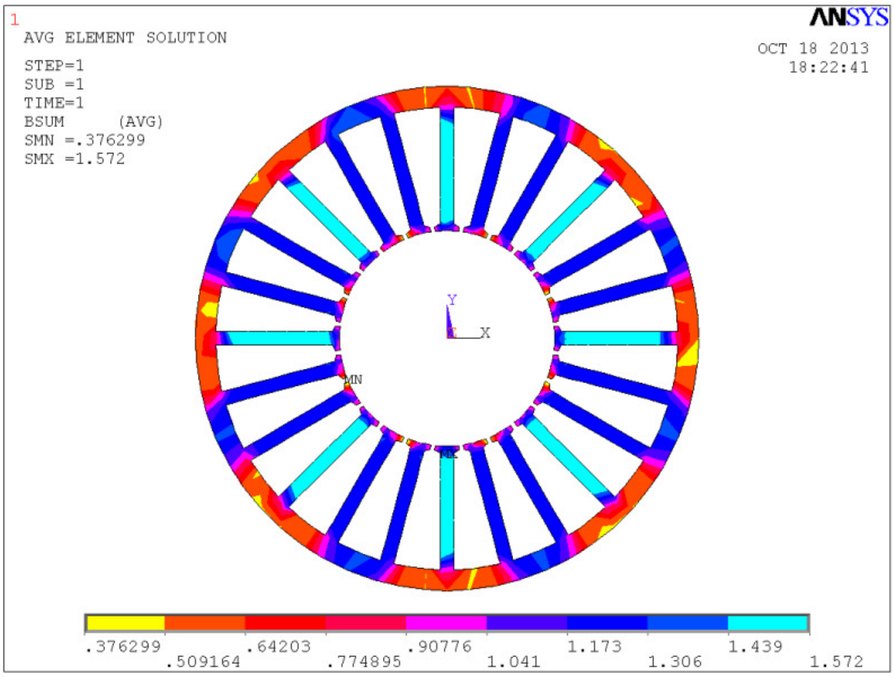

Fig. 3 No load flux density in the stator core

The maximum flux density in the stator teeth, stator back iron and rotor back iron are 1.572 T, 1.439 T and 1.808 T respectively. Since all the values are less than 1.9T there is no saturation in the stator and rotor core at no load.

Magnet operating point is important, because it defines the utilisation of the magnet. By calculating the magnet flux density and magnetising force the operating point and load line can be drawn. The magnet operating point should be such value that it should not demagnetise the magnet in the presence of external field and temparature variation. The magnet flux density profile and demagnetising force offered to magnet at no load due to airgap and slot structure is shown in the Fig. 4 and Fig. 5 respectively. Magnet operating point is shown in Fig. 6. It can be concluded that the operating point is within the set limits.

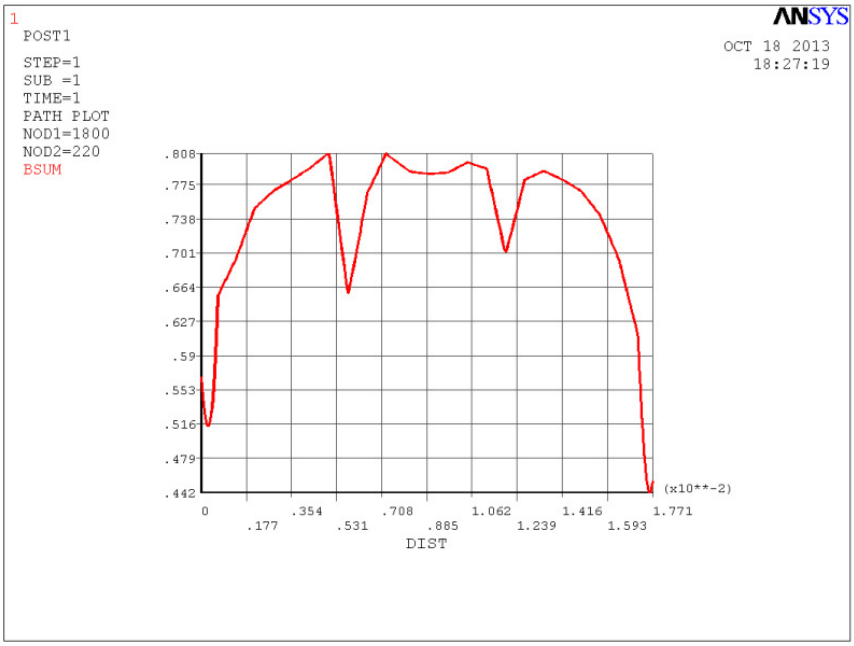

Fig. 4 Magnet flux density at no load

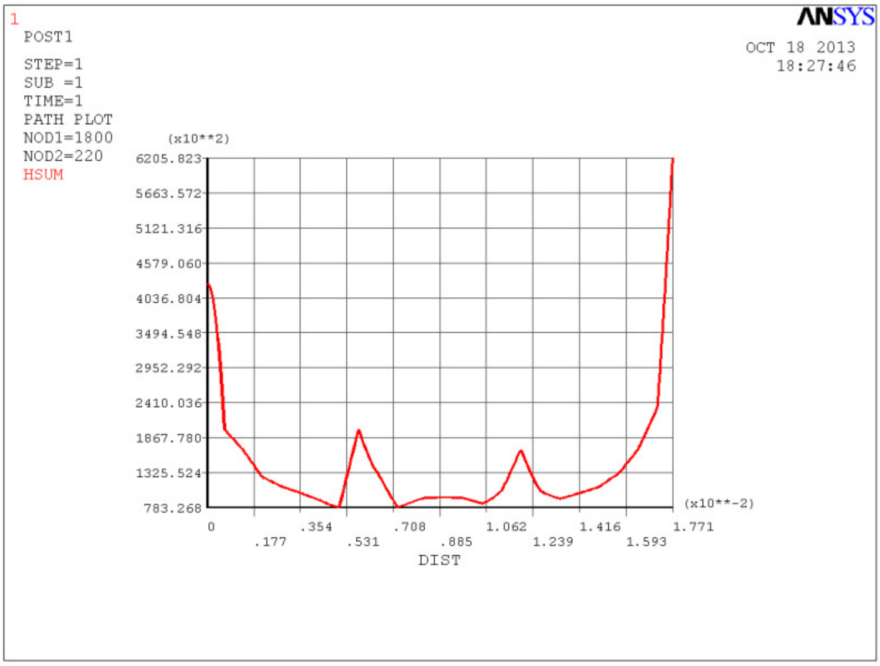

Fig. 5 Demagnetising force offered by magnet at no load

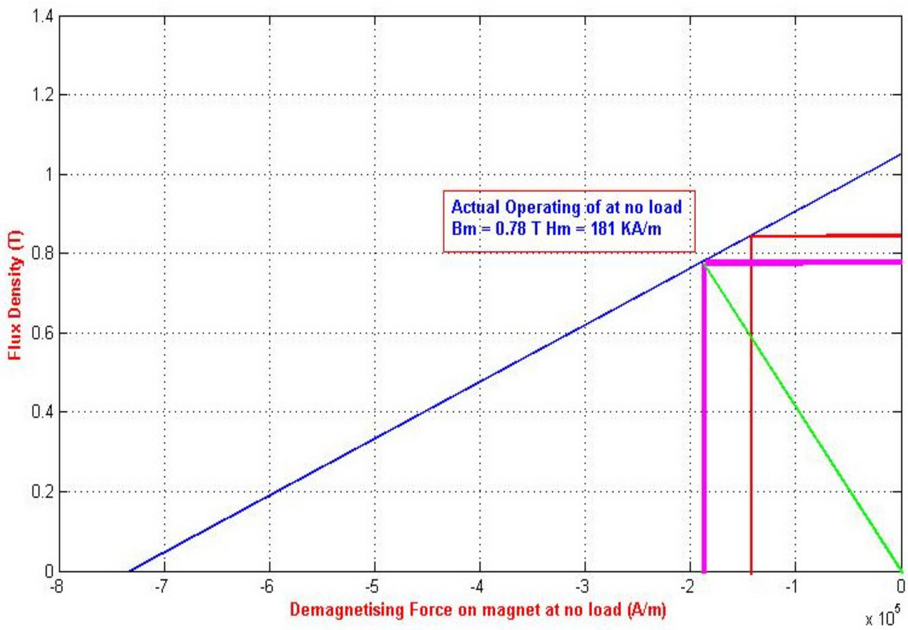

Fig.6 Magnet operating point as per non linear analysis

7. Finite Element Analysis under load condition

The Finite Element Analysis is carried out on load to analyse the effects of armature reaction. The effect of armature reaction can be seen by deriving the magnet operating point on load. The distortion of flux can be found from the flux profile of the airgap at load.The effect of armature reaction can be classified into d- axis and q- axis effects. Assuming that Phases R and B are conducting at an instant the slot current polarities are fed in to the model as shown in Fig. 7.

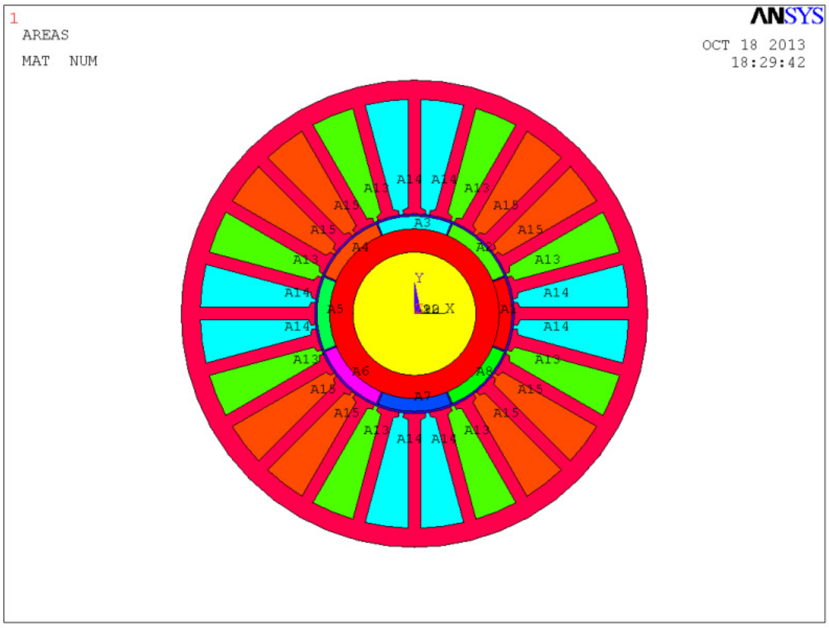

Fig. 7 Phase wise current distribution at an instant in the stator

Various plots of flux, flux density and flux density profile of the motor under load condition are shown from Fig. 8 to Fig.10. Air gap flux profile under one pole arc is shown in Fig. 8 reveals that the armature reaction distorted the no load flux profile. It aided the magnet flux at some places and reduced at some.

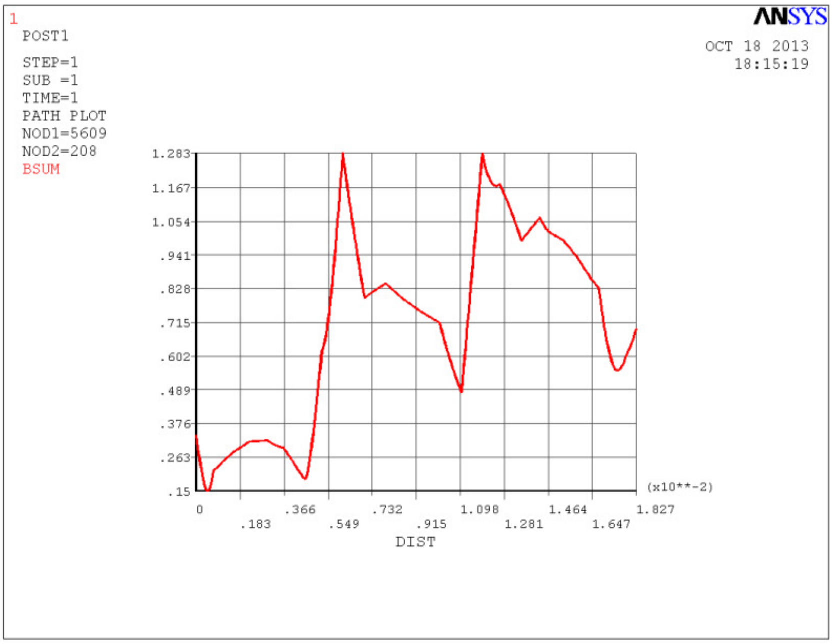

Fig . 8 Airgap flux density due to crossmagnetisation on load

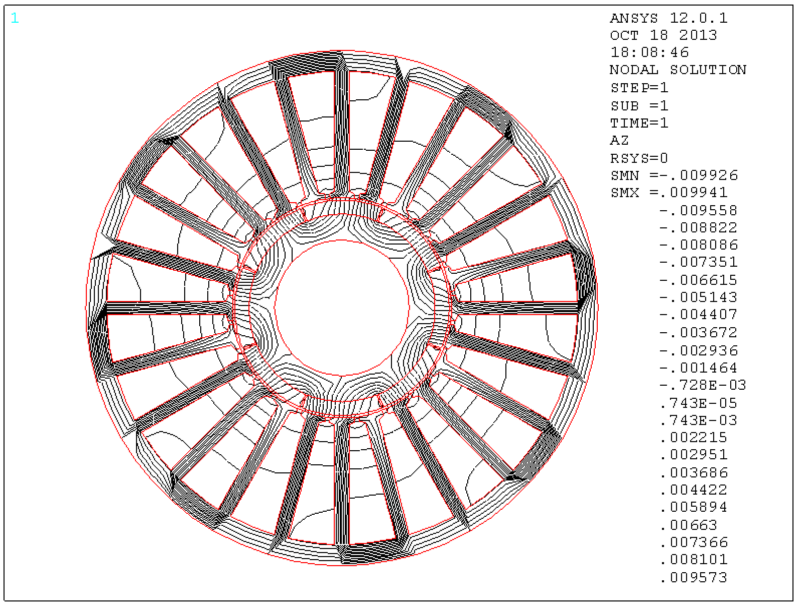

Fig.9 Flux profile of the stator on load

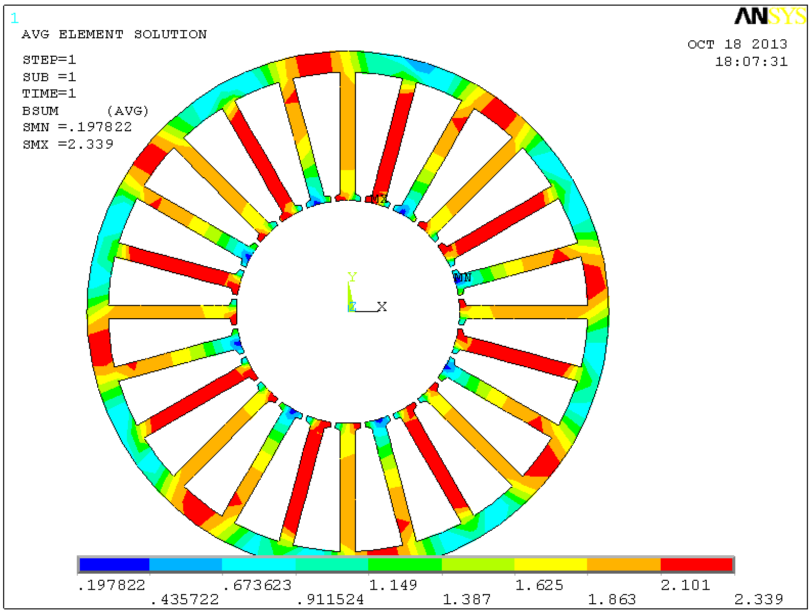

Fig. 10 Flux density profile of stator at full load

From the above Fig the maximum flux density in stator back iron and stator teeth are 2.339 T and 2.339 T respectively. Demagnetization which may occur in extreme conditions like short circuit. In such a condition, armature flux is in direct opposition to direct axis rotor magnetic flux axis. The airgap flux density,magnet flux density and magnetic field intensity are shown in Fig.11, Fig. 12 and Fig.13 respectively.

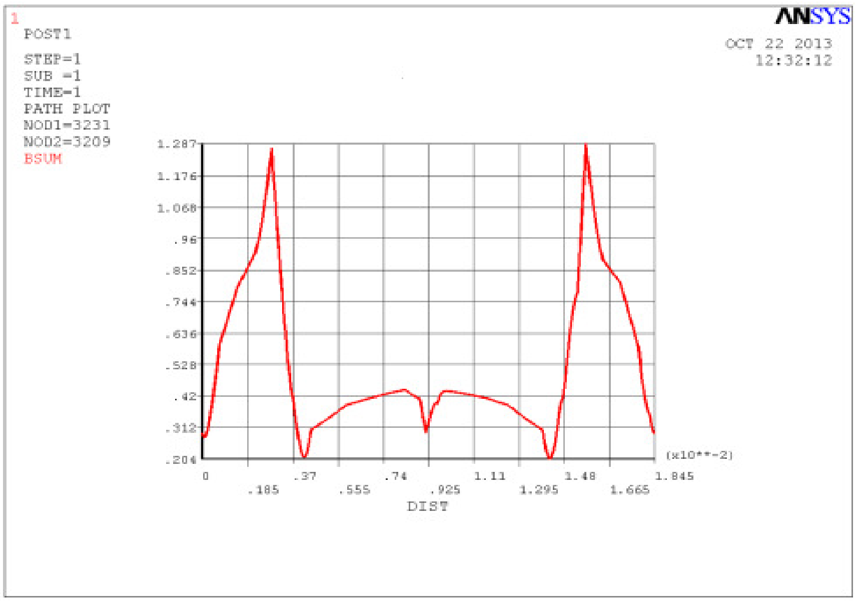

Fig. 11 Air gap Flux density under demagnetising conditions

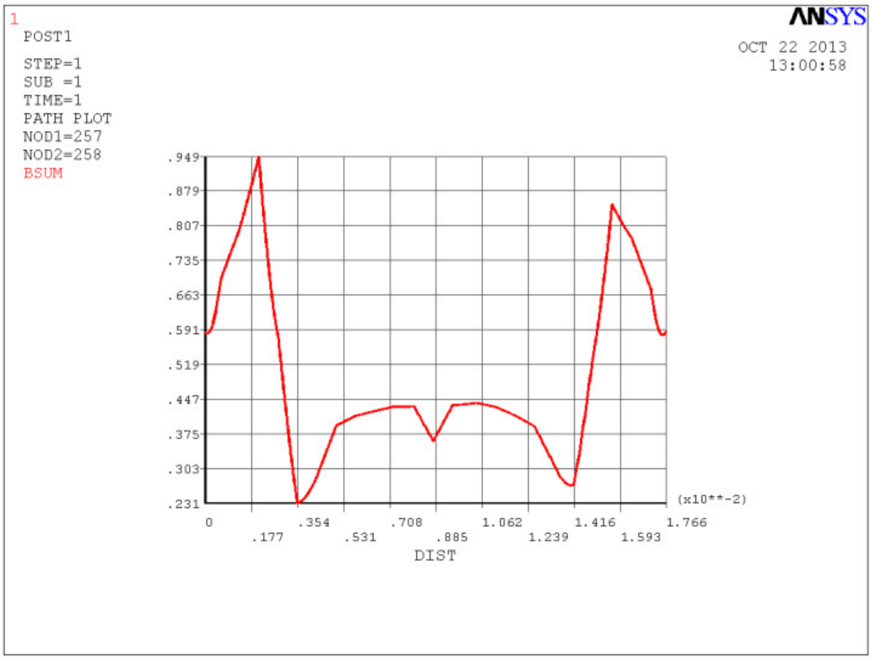

Fig. 12 Magnet flux density during demagnetisation.

The operating point in this condition is shown in Fig. 14

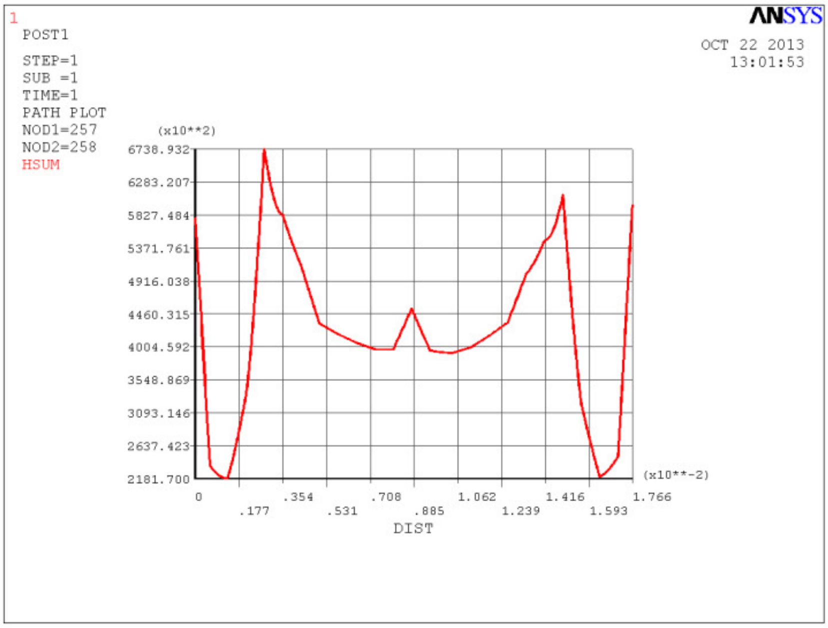

Fig. 13 Magnet field intensity under demagnetising condition

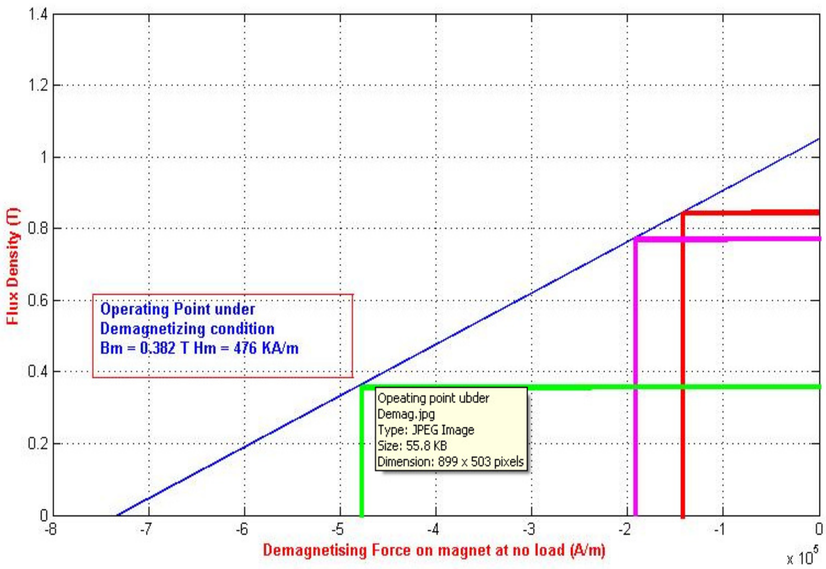

Fig. 14 Magnet operating point under demagnetising condition

8. Speed Torque Characteristics of the Motor.

The equations governing the motor operation are

$$V = I_a R_a + E_b \tag{8}$$

$$E_b = K_b \times \omega \tag{9}$$

$$T = K_t \times I_a \tag{10}$$

Solving these equations gives the relation between speed torque as

$$\omega = \frac{V}{K_b} - \frac{T}{K_b K_t} R_a \tag{11}$$

Solving the Eq. 11 gives the speed torque characteristic of motor. The no load speed torque plot is shown in Fig.15. The peak torque will be limited in the current limit of the controller.

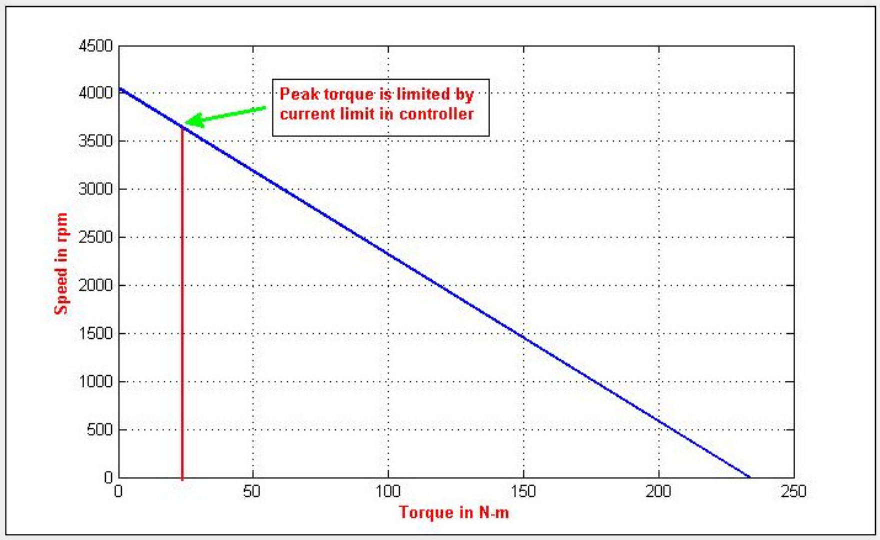

Fig. 15 Ideal Speed Torque plot

The torque data obtained from FE analysis and the corresponding plot indicate the non-linearity in the Torque vs current characteristic on load, which is due to saturation in motor due to armatur reaction.Torque data is shown in Table 4. Torque speed characteristics are shown in Fig. 16.

Table. 4 Load torque data from FEA

S no	Current loading In A/mm^2	Torque from FEM in N-m/m	Motor Torque in N-m (N-m/m x Li x Kst)
1	1	49.80	4.7
2	2	97	9.1
3	3	138	12.9
4	4	176	16.5
5	5	213	19.9
6	6.7	270	25.3

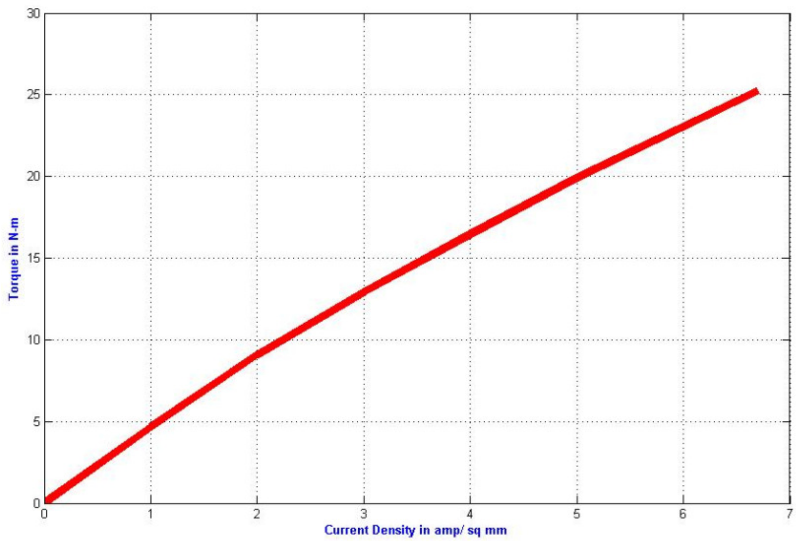

Fig.16 Torque Current chararacteristic of motor (from Non Linear Analysis)

The design output is summerised as follows in Table 5

Table. 5 Motor design Parameters

S.No	Parameter	Description	Value
1	D_{so}	Stator Outer Diameter	110 mm
2	D_{sb}	Stator diameter at slot bottom	101 mm
3	D_{si}	Stator inner diameter	47 mm
4	D_{ro}	Rotor outer diameter	23 mm
5	W_{bi}	Width of stator/rotor back iron	4.5 mm
6	W_{tb}	Width of the teeth	3 mm
7	l_m	Length of the magnet	3 mm
8	θ_p	Magnet pole arc	44°
9	g	Length of air gap	0.5 mm
10	(B_m, H_m)	Operating point	0.87T,140A/m
11	R_{ph}	Armature Resistance/ph	0.011 ohms
12	L_{ph}	Armature Inductance /ph	0.197 mH
13	I_a	Armature current (peak)	125 A
14		Cu Loss	89 W
15		Iron Loss	40 W
16	K_b	Back emf constant	0.2 v/rad/sec
17	K_t	Torque constant	0.2 N-m/A
18	ΔT	Temparature rise	74.34°C

9. Conclusion

The design of the BLDC motor was carried out to meet the given specification. The design covered sizing of the motor, conventional magnetic design to arrive at preliminary magnetic parameters of the motor, electrical parameters and performance characteristics. The design also includes the analysis of motor with FE analysis to include the non-linear magnetic properties of the material. FE analysis was carried out on no-load and on load to calculate magnetic parameters to validate the conventional design results.

The analysis also included study of armature reaction effects on the magnetic design and performance of the motor. The parameters obtained from the analytical design and FE analysis state that the motor meets the required specifications.

References

[1] Duane C Hanselman, Brushless Permanent Magnet Motor Design, McGraw-Hill, 1994

[2] Jack F Gieras, Mitchell Wing Permanent Magnet Motor Technology, Macel Dekker, 2002

[3] Lakshminarayana, Tarakalyani and Ravindranath, Design of a compact BLDC motor for High power, High Bandwidth Rotary Electro-Mechanical Actuator for Aerospace Application, *Annual IEEE India Conference (INDICON),* 1-4, 2011.

[4] M.Norhisam, A. Nazifah, I. Aris, H. Wakiwaka, Effect of Magnet Size on Torque Characteristic of Three Phase permanent Magnet Brushless DC Motor *IEEE Student Conference on Research and Development (SCOReD),* 293 – 296, 2010.

[5] In-Soung Jung, Ha-Gyeong Sung, Yon-Do Chun & Jin-Hwan Borm, Magnetization Modeling of a Bonded Magnet for Performance Calculation of Inner-Rotor Type BLDC Motor, *IEEE Transactions on Magnetics,37(4),* 2810 – 2813, 2001.

[6] Hong-Soon Chang and Soo-Hyun Baek, Finite Element Analysis of an Anisotropic Ferrite Bonded Magnet for BLDC Motor Design, *Proceedings of Fifth International Conference on Electrical Machines and Systems, ICEMS, 2,* 1170 – 1173, 2001.